Carbohydrate Polymers 85 (2011) 261–267

Contents lists available at ScienceDirect

Carbohydrate Polymers

journal homepage: www.elsevier.com/locate/carbpol

In situ-forming chitosan/nano-hydroxyapatite/collagen gel for the delivery of bone marrow mesenchymal stem cells

Zhi Huang[a,1], Bo Yu[b,1], Qingling Feng[a,*], Songjian Li[b], Yan Chen[c], Luqiao Luo[d]

[a] State key Laboratory of New Ceramics and Fine Processing, Department of Materials Science and Engineering, Tsinghua University, Beijing 100084, China
[b] Department of Orthopedics, Zhujiang Hospital of Southern Medical University, Guangzhou 510282, China
[c] Department of Ultrasonic Diagnosis, Zhujiang Hospital of Southern Medical University, Guangzhou 510282, China
[d] Department of Pathology, Zhujiang Hospital of Southern Medical University, Guangzhou 510282, China

ARTICLE INFO

Article history:
Received 14 December 2010
Received in revised form 13 February 2011
Accepted 14 February 2011
Available online 22 February 2011

Keywords:
In situ-forming
Injectable
Bone marrow mesenchymal stem cells
Biocompatibility

ABSTRACT

A biomimetic and thermosensitive gel scaffold was prepared from chitosan (CS), nano-hydroxyapatite (HA) and collagen (Col). The changes of storage modulus, loss modulus, pH and conductivity of the CS/HA/Col system as a function of temperature confirmed the liquid-to-gel phase transition process occurred under physiological conditions. The formed gel acted as a biocompatible substrate for the proliferation of rat bone marrow stem cells (rBMSCs) *in vitro*. rBMSCs suspension was co-injected with CS/HA/Col solution into Wistar rats. The injected rBMSCs survived in the CS/HA/Col gel for 28 days *in vivo*. The CS/HA/Col/rBMSCs gels induced less inflammatory reaction in the host tissue than the CS/HA/Col gels. Our results suggest that the CS/HA/Col system can be used to load rBMSCs *in vitro* homogeneously. The CS/HA/Col system can be injected into body in a minimally invasive manner and provides a biocompatible environment for rBMSCs survival *in vivo*.

1. Introduction

Natural bone is a complex biomineralized composite mainly containing hydroxyapatite (HA) and collagen (Col) with an intricate hierarchical structure (Li, Feng, Wang, & Cui, 2006). Weiner and Wagner depicted the hierarchical organization of natural bone as follows: the nano-structured array of HA crystals with their *c*-axis aligned with the long axis of the collagen fibrils, which associated as bundles and aligned along their long axis (Palmer, Newcomb, Kaltz, Spoerke, & Stupp, 2008; Weiner & Wagner, 1998).Chitosan (CS) is a cationic linear polysaccharide from crab and shrimp shell (Li & Feng, 2005b; Ma et al., 2010; Muzzarelli, 2009). Chitosan-based thermosensitive hydrogel has been widely investigated and utilized in cell encapsulation and tissue engineering (Ji et al., 2010; Ma et al., 2010; Zhao et al., 2009). In our preliminary study, a new type of thermosensitive material based on CS, HA and Col was fabricated with a biomimetic strategy (Huang, Feng, Yu, & Li, 2011). HA/Col uniformly dispersed in the chitosan matrix and this CS/HA/Col composite showed some features of natural bone both in main composition and hierarchical structure as proposed by Weiner & Wagner (1998).

The aim of this paper was to characterize the thermosensitive properties of the CS/HA/Col system using rheological measurements. More importantly, we seeded the rat bone marrow mesenchymal stem cells (rBMSCs) in CS/HA/Col gel both *in vitro* and *in vivo* to evaluate the cell delivery ability of the gel.

2. Materials and methods

2.1. Materials

Type I collagen (medical grade) from calf skin was purchased from YierKang Company (China). Chitosan (water content < 10%; ash content < 1.0%) was obtained from Shandong AK Biotech Ltd., China. The degree of deacetylation of chitosan as estimated by colloidal titration with potassium poly(vinyl sulfate) (Cho, Heuzey, Begin, & Carreau, 2005) was 96% and the molecular weight of chitosan determined by size exclusion chromatography (Cho et al., 2005) using dextran as standards was $\sim 2.5 \times 10^5$ Da. Hydrated β-glycerophosphate disodium salt ($C_3H_7O_3PO_3Na_2 5H_2O$; $M_w = 306$) was purchased from Sigma Chemical Co. (US). All other reagents were of suitable analytical grade.

2.2. Preparation of CS/HA/Col

The CS/HA/Col composite was prepared by the procedure reported previously (Huang et al., 2011). Firstly, HA/Col powder was

* Corresponding author. Tel.: +86 10 62782770; fax: +86 10 62771160.
E-mail address: biomater@mail.tsinghua.edu.cn (Q. Feng).
[1] Zhi Huang and Bo Yu contributed equally to this work.

0144-8617/$ – see front matter © 2011 Elsevier Ltd. All rights reserved.
doi:10.1016/j.carbpol.2011.02.029

synthesised by self-assembly of nano-fibrils of mineralized collagen (Zhang, Liao, & Cui, 2003) and sterilized by γ-ray irradiation (1.5 Mrad). Secondly, chitosan (2 g) was dissolved in hydrochloric acid solution (98 mL, 0.1 M). Thirdly, the HA/Col powder was added to the chitosan solution (0.02 g/mL). Finally, the pH of the CS/HA/Col solution was adjusted to 7.0 by adding droplets of β-glycerophosphate solution [30% (w/v)]. The samples for biological tests were prepared in line with the aseptic technique in an aseptic manipulation cabinet.

2.3. Rheological measurements

Rheological measurements were carried out on Physica MCR300 Modular Compact Rheometer (Anton Paar, Germany) according to the method described by Jaepyoung et al. (Cho et al., 2005; Li & Feng, 2005a).

2.4. pH and conductivity measurements

To follow up the heat-induced gelation process, pH (pH meter, METTLER TOLEDO, US) and conductivity (DDS-12A, Shanghai Pengshun Scientific Instrument Co., Ltd., China) values were recorded in a continuous manner as a function of temperature (Cho, Heuzey, Begin, & Carreau, 2006).

2.5. rBMSCs isolation

The rBMSCs were harvested from the femurs of female Wistar rats (80–100 g) according to the methods previously reported (Akahane et al., 1999; Cho et al., 2008; Ohgushi, Goldberg, & Caplan, 1989). The third passage of rBMSCs was used. For implantation experiments, the rBMSCs were labeled by incubation for 48 h at 37 °C using the bromodeoxyuridine (BrdU, Sigma, USA) according to the manufacturer's instructions.

2.6. In vitro cytocompatibility study

The CS/HA/Col gels were prepared by pipetting the CS/HA/Col solution (50 μL per well) into clean 24-well plates and incubated at 37 °C for 1 h. rBMSCs (3×10^4 cells per well) were then seeded on the surface of the CS/HA/Col gels. For the control group, the same number of rBMSCs was seeded on a clean 24-well plate. All the plates were incubated at 37 °C in a humidified 5% CO_2 atmosphere cell-culture incubator. Fresh basic culture medium (DMEM supplemented with 10% fetal bovine serum) was carefully changed every 2 days.

To assess the percentage of living cells on the CS/HA/Col gel, a quantitative colorimetric assay using a CCK-8 kit (Cell Count Kit-8, Beyotime, US) was used. After 2, 7, 15 and 20 days of culture, CCK-8 reagent (100 μL) was added to rBMSCs in 1 mL medium per well. The plates were incubated at 37 °C for 4 h and shaken for 1 min. 100 μL of liquid from each well was transferred to a 96-well plate and absorbance (OD value) at 450 nm was measured using a microplate reader (WellScan MK22, Labsystems, Finland). The relative cell growth (RCG) was presented as:

$$\mathrm{RCG} = \frac{\mathrm{OD_e}}{\mathrm{OD_c}} \times 100\% \quad (1)$$

OD_e was the mean OD values of the CS/HA/Col at the different time points, and OD_c was the mean OD values of the control group at 2 days after initial seeding. The viability of control cells at 2 days after initial seeding was defined as 100% viability (Baruch & Machluf, 2006; Zhao et al., 2009). All measurements were performed four times.

2.7. Alkaline phosphatase staining

On day 15, alkaline phosphatase activity (ALP) was detected by ALP staining according to methods previously reported (Kim et al., 2008). The samples were washed with phosphate buffered saline (PBS) and fixed with paraformaldehyde (4%) supplemented with cacodylic acid (0.1 M, Sigma) for 10 min. After washing with cacodylic acid, ALP solution (Sigma) was added and incubated at 37 °C for 1 h. Finally, the samples were washed with distilled water for three times.

2.8. Implantation experiments in rats

All the animals were operated according to the guidelines for animal experiments. In this study, eighteen female Wistar rats (80–100 g) were randomly divided into two different treatment groups: one group was CS/HA/Col gel only (G1, 0.5 mL gel only); the other was CS/HA/Col gel with rBMSCs (G2, 0.5 mL gel + 5×10^6 rBMSCs). The G2 solutions were prepared by gently mixing a pellet containing 5×10^6 newly isolated rBMSCs with 0.5 mL of CS/HA/Col solution. A 1-mL syringe with a 26-gauge needle was used to inject the solution into the subcutaneous dorsum of a rat.

2.9. Histological analysis

Gels with surrounding tissues were dissected and removed from the subcutaneous dorsum on day 1, day 14 and day 28 post implantation. Each gel was fixed with 10% buffered formalin and embedded in paraffin. The embedded gels were sectioned into 4 μm thick sections, and the sections were deparaffinized, hydrated and routinely stained with hematoxylin eosin and BrdU. The staining of BrdU was according to the method previously reported (Ahn et al., 2009; Axelsson, Akbarshahi, Said, Malmstrom, & Andersson, 2010). The deparaffinized sections were washed with PBS and incubated in hydrogen peroxide (3%, in PBS) for 10 min, followed by washing three times with PBS. The sections were incubated with hydrochloric acid (2 N) for 30 min at 37 °C and neutralized with boric acid (pH = 8.5). Monoclonal anti-BrdU antibody (Abcam, Cambridge, MA) was applied for 40 min. The single stained section was washed, and then second antibody (Envision kit; Dako) was applied for 40 min. To show the BrdU-positive cells, the sections were washed with PBS, visualized using 3,3-diaminobenzidine-tetrahydrochloride (DAB, Envision kit; Dako) and counterstained with hematoxylin.

3. Results and discussions

3.1. Thermosensitive properties of the CS/HA/Col system

The changes in rheological behavior of CS/HA/Col system upon temperature increase and decrease were depicted in Fig. 1. The heating process can be divided into four stages according to the slope of the curve. In region 1, both G' and G'' moduli decreased with increasing temperature. In region 2, both G' and G'' moduli gradually increased from about 27 °C while the sample was still flowable. In region 3, both G' and G'' moduli increased rapidly. However, the growth rate of G' modulus was much larger than that of G'' modulus in this region. In region 4, both G' and G'' moduli eventually reached the onset of plateaus at about 50 °C, which corresponded to the formation of a gel.

To investigate the heat-induced gelation process, a non-isothermal kinetic model has been developed by combination of Arrhenius and time-temperature relationships using G' modulus

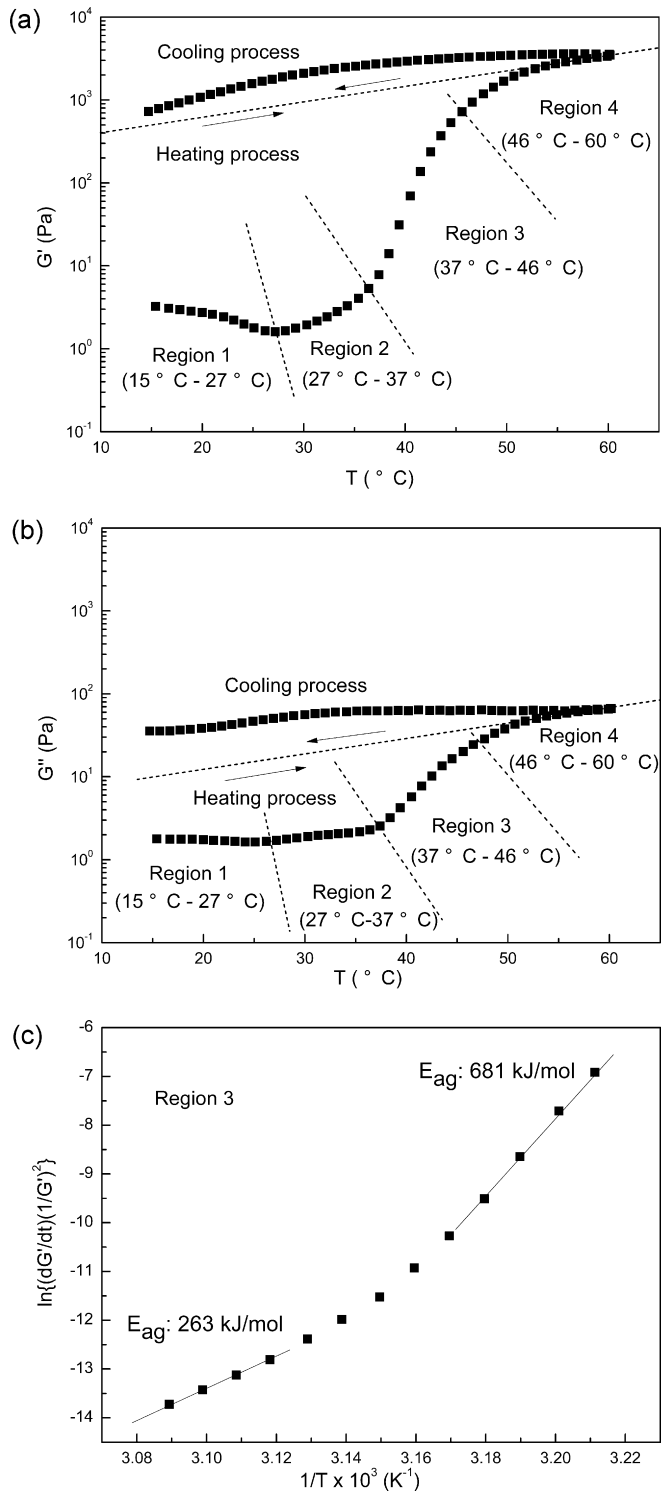

Fig. 1. Rheology: temperature sweeps. Storage modulus G' (a) and loss modulus G'' (b) of the CS/HA/Col system, reported as a function of temperature (±1 °C/min, $\omega = 6.28$ rad/s, $\gamma_0 = 0.01$) and (c) nonisothermal gelation kinetics of the CS/HA/Col system in region 3 (37–50 °C).

(Cho et al., 2006, 2005):

$$\ln\left(\frac{1}{G'^2}\frac{dG'}{dt}\right) = \ln k_0 + \frac{E_{ag}}{RT} \quad (2)$$

where G' is the storage modulus (Pa), k_0 is the Arrhenius frequency factor, t is the time (s), E_{ag} is the activation energy for gelation, T is the absolute temperature and R is the gas constant (8.314 J mol^{-1}K^{-1}).

Eq. (2) was used to estimate the activation energy during the gelation process for the CS/HA/Col system by plotting: $\ln\left(\frac{1}{G'^2}\frac{dG'}{dt}\right)$ vs $\frac{1}{T}$ and taking the slope as E_{ag}. The values of activation energy decreased as the temperatures increased from 37 °C to 50 °C (Fig. 1(c)). This result indicated that the development of three dimensional physical network of CS/HA/Col hydrogel was energetically easier at higher temperature.

To investigate the thermoreversibility of the CS/HA/Col system, the formed gels were cooled down from 60 to 15 °C. As shown in Fig. 1, both G' and G'' moduli gradually decreased in the cooling process, however, G' modulus remained larger than G'' modulus even at the lowest temperature (15 °C), which indicated that the CS/HA/Col gel was partially thermoreversible.

The pH (Fig. 2(a)) and conductivity (Fig. 2(b)) of the CS/HA/Col system were simultaneously measured as functions of temperature. As shown in Fig. 2(a), the pH values decreased linearly with increasing temperature, which was due to the deprotonation of chitosan upon heating (Lavertu, Filion, & Buschmann, 2008). However, the pH values remained in a physiologically acceptable level from 7.2 to 6.5.

As observed in Fig. 2(b), the conductivity of the CS/HA/Col system increased linearly with temperature in the heating process. Conductivity relates to the ionic concentration and the strength of the solution. Heating induced transfer of protons from chitosan to solution and decreased the pH value and the ionic strength (Cho et al., 2005), thereby conductivity increased as a function of temperature.

Gel formation mechanisms and dynamics dictate how cells are incorporated into a scaffold and how the scaffold is then delivered into the body (Drury & Mooney, 2003). In the present work, our results suggested that the gelation of the CS/HA/Col solution induced by heating was the result of a progressive reduction of the degree of ionization of chitosan. As the temperature increased, protons transferred from chitosan to solution, reducing the electrostatic repulsion between the chitosan chains and inducing the attractive forces such as hydrophobic and hydrogen bonding to form a gel.

The temperature and pH should not be significantly altered during the gelation process for the *in situ*-forming system (Hou, De Bank, & Shakesheff, 2004). Our results indicated that the CS/HA/Col system underwent gelation triggered by a change in temperature. The gelation temperature could be determined from the crossover point of the G' and G'' moduli (Cho et al., 2005), and for CS/HA/Col system the gelation temperature was at around 31 °C (Fig. 1), which indicated that the CS/HA/Col system could undergo thermal gelation at body temperature. The pH values also remained in a physiologically acceptable level during the gelation process.

3.2. Characterization of the gel strength

Fig. 3 illustrates the rheological behavior of CS/HA/Col system against small amplitude oscillatory shear before gelation and after gelation at 15 °C. Before gelation, the CS/HA/Col system behaved like a typical viscoelastic polymer solution, i.e. both G' and G'' moduli gradually increased with the frequency, and G'' modulus was larger than G' modulus. However, after gelation and cooling to 15 °C, the CS/HA/Col system showed a typical gel-like behavior, i.e. both G' and G'' moduli were less dependent on the frequency over the whole frequency range and G' modulus was larger than G'' modulus. This also indicated a strong and stable gel and its non complete thermoreversibility (Chenite, Buschmann, Wang, Chaput, & Kandani, 2001; Lessard, Ousalem, Zhu, Eisenberg, & Carreau, 2003).

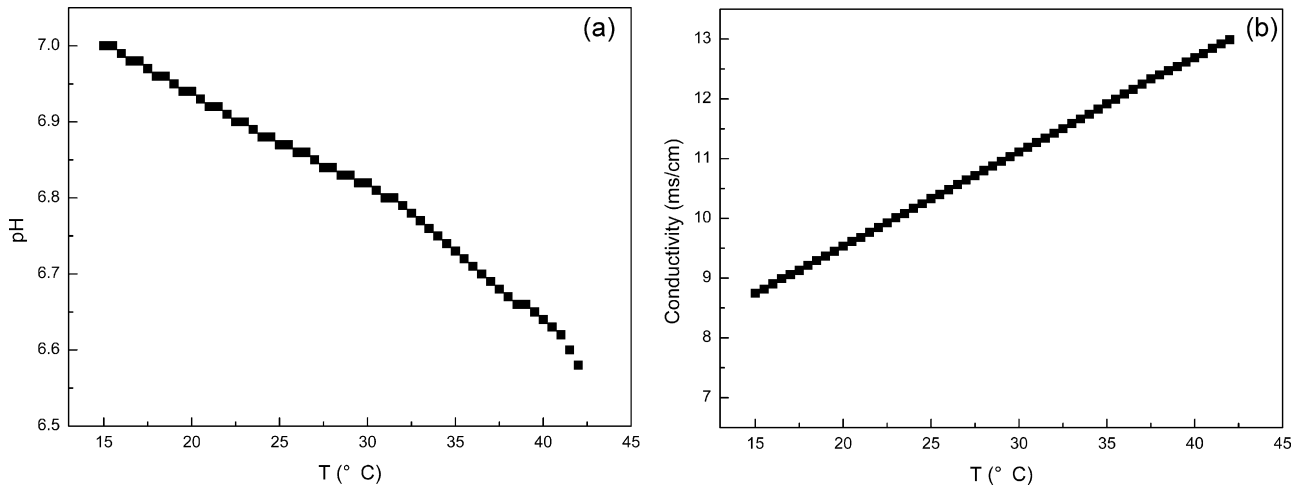

Fig. 2. Variation of the pH (a) and conductivity (b) of the CS/HA/Col system with temperature in the heating process (1 °C/min).

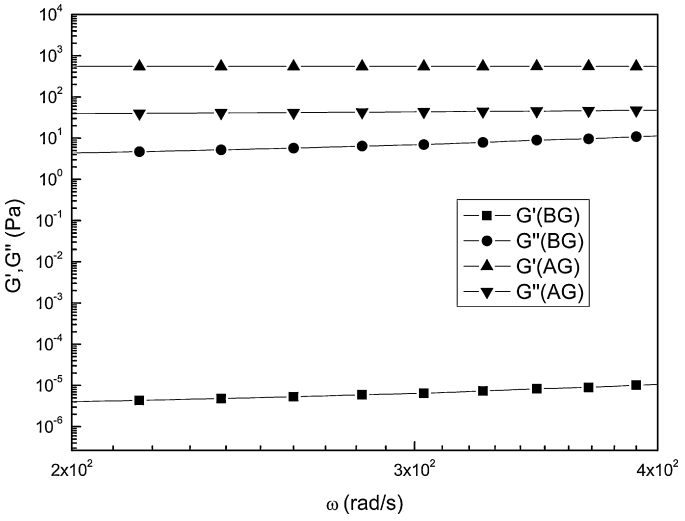

Fig. 3. Rheology: frequency sweeps before gelation (BG) and after gelation (AG) at 15 °C (γ_0 = 0. 1). Storage modulus (G') and loss modulus (G'') are plotted against the frequency for the CS/HA/Col system.

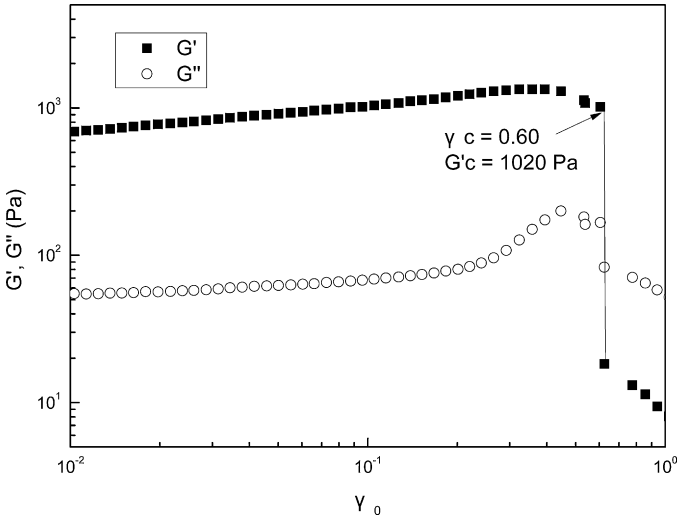

Fig. 4. Rheology: strain sweep resulting in gel breakup. G' and G'' as functions of strain amplitude (γ_0) for the CS/HA/Col system (ω = 6.28 rad/s).

The effect of strain on the CS/HA/Col gel obtained at an isotherm of 37 °C is shown in Fig. 4. G' modulus decreased rapidly at strain larger than 0.60 where the gel broke up. The critical strain (γ_c), at which a polymeric system shows nonlinear viscoelastic behavior, can be used to calculate the cohesion energy (Cho et al., 2005; Lessard et al., 2003):

$$E_c = \frac{1}{2}\gamma_c G'^2_c \quad (3)$$

E_c and G'_c are the cohesion energy and the storage modulus at the critical strain, respectively. In this study, a cohesion energy value of approximately 187 J/m^3 was calculated for CS/HA/Col gel at 37 °C. The cohesion energy is related to the energy required for the formation of physical cross links between the polymer chains (Cho et al., 2005; Lessard et al., 2003).

Cells encapsulated within a gel respond to applied mechanical deformation/strains non-uniformly (Bryant, Anseth, Lee, & Bader, 2004). Dynamic mechanical analysis provides quantitative information on the rheological and viscoelastic properties of a material (Anseth, Bowman, & BrannonPeppas, 1996). Monitoring the dynamic mechanical properties is also important to answer biologically important questions and improve on the design of hydrogel carriers for cell delivery (Kloxin, Kloxin, Bowman, & Anseth, 2010). The dynamic mechanical properties of CS/HA/Col system were studied by frequency sweep and strain sweep experiments. The frequency sweep experiments confirmed the thermal-sensitivity of the CS/HA/Col system and its non complete thermoreversibility. Before gelation, the CS/HA/Col solution was flowable and injectable. After gelation, the CS/HA/Col gel showed good stability against high frequency. In the strain sweep experiments, G'_c was evaluated as 1020 Pa and E_c was calculated as 16 kJ/mol. These values were almost four times higher than that obtained for a 2 wt% chitosan gel (Cho et al., 2005). A possible explanation is that the interactions between collagen in HA/Col and chitosan may occur by hydrogen bonds formation (Chen, Mo, He, & Wang, 2008; Sionkowka, Wisniewski, Skopinska, Kennedy, & Wess, 2004), which can bind the chitosan and HA/Col together. This likely contributed to a higher elastic modulus and cohesion energy for the CS/HA/Col gel.

3.3. *In vitro cytotoxicity assays*

After culturing with basic culture medium for 15 days, we found that rBMSCs cultured on the CS/HA/Col gel showed negative for the ALP staining (data not shown), which indicated that rBMSCs cultured on the CS/HA/Col gel with basic culture medium did not show

osteogenic characteristics. Various growth factors and cytokines are responsible for differentiation of stem cells (Dawson, Mapili, Erickson, Taqvi, & Roy, 2008). Therefore, rBMSCs cultured on the CS/HA/Col gel with basic culture medium did not differentiate into osteoblast for the lack of growth factors or cytokines, such as bone morphogenetic protein.

The RCG values were 80.6 ± 4.0 (day 2), 72.8 ± 1.3 (day 7), 94.8 ± 3.2 (day 10), 95.5 ± 2.3 (day 15) and 106.5 ± 3.5 (day 20), which indicated that the CS/HA/Col gel was cytocompatible with rBMSCs, and rBMSCs on the CS/HA/Col gel could keep their self-renew and proliferative activities for up to 20 days.

3.4. Subcutaneous implantation

The feasibility of using CS/HA/Col system as *in situ* gel-forming scaffold for cell delivery was examined in Wistar rats. The CS/HA/Col solution with appropriate mixtures of rBMSCs was injected into the subcutaneous dorsum of a Wistar rat with a 1-mL syringe (Fig. 5(a)). Gel formed *in situ* after injection and maintained *in situ* for at least 28 days (Fig. 5(b)). The BrdU-stained sections of gel implants with rBMSCs (G2 gel, Fig. 6) showed a number of rBMSCs (dark brown) interspersed in the gel matrices. This result demonstrated that the rBMSCs had survived inside the gel at the injection site for at least 28 days.

Fig. 7 shows hematoxylin and eosin stained sections of gel implants with surrounding tissues after 1, 14 and 28 days. As shown in the Fig. 7(a and b), G1 gels elicited more notable acute inflammatory reaction (infiltrated with neutrophils and granulocytes) than G2 gels on day 1. On day 14, both gels exhibited host tissue responses, with accumulations and recruitment of inflammatory cells that contained macrophages, lymphocytes, and rarely giant cells (Anderson, 2001). However, the inflammatory reaction for the G2 gels was significantly less than G1 gels (Fig. 7(c and d)). From 14 to 28 days, the degree of inflammatory reaction for the G2 gels declined significantly. However, the inflammatory cells surrounding the G1 gels were still abundant. Recently, BMSCs have been shown to display immunosuppressive properties on T-lymphocyte proliferation (Bartholomew et al., 2002; Di Nicola et al., 2002; Djouad et al., 2003). This indicated that the immunosuppressant properties of rBMSCs were valuable in improving the biocompatibility and successful application of *in situ*-forming CS/HA/Col gels.

No osteoid matrix was visible in any sample, which confirmed that osteogenesis did not proceed when rBMSCs were injected subcutaneously without the addition of osteoinductive factor (Yoshikawa, Ohgushi, & Tamai, 1996). In this regard, addition of other growth factors was required to induce rBMSCs differentiation and for ultimately formation of a variety of different tissue types (Dawson et al., 2008).

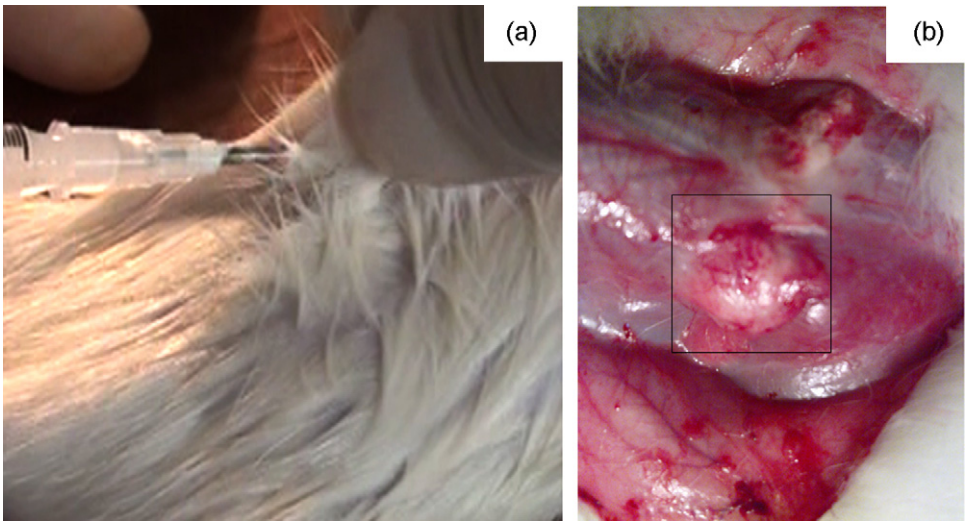

Fig. 5. *In situ* formation of the CS/HA/Col gel: (a) subcutaneous injection of the CS/HA/Col solution and (b) the *in situ* formed gel 4 weeks after injection.

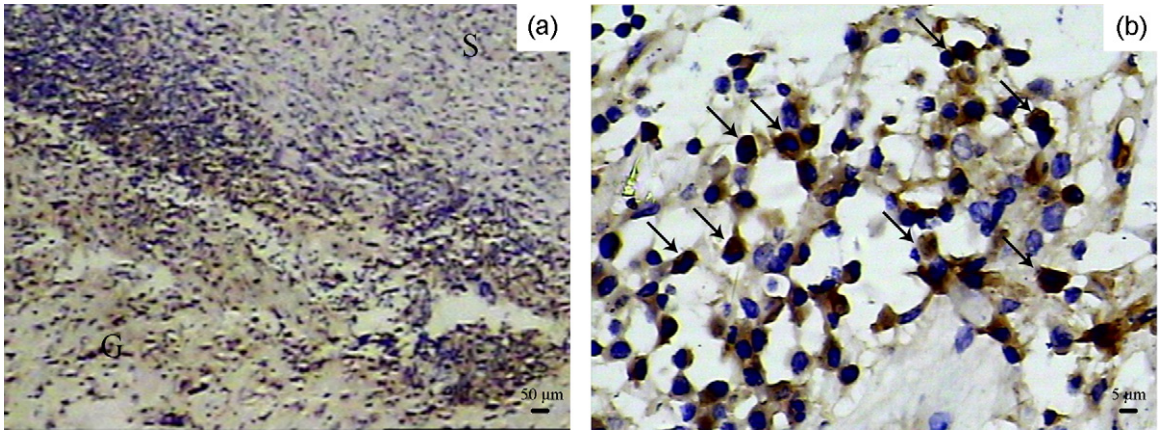

Fig. 6. Light photograph of BrdU-stained histological sections of the G2 gel after 28 days. rBMSCs were labeled with BrdU and the BrdU-positive rBMSCs (arrows) demonstrate that rBMSCs survive inside the gel at the injection site for at least 28 days. G: gel, S: surrounding tissues. Magnification: (a) 40× and (b) 400×.

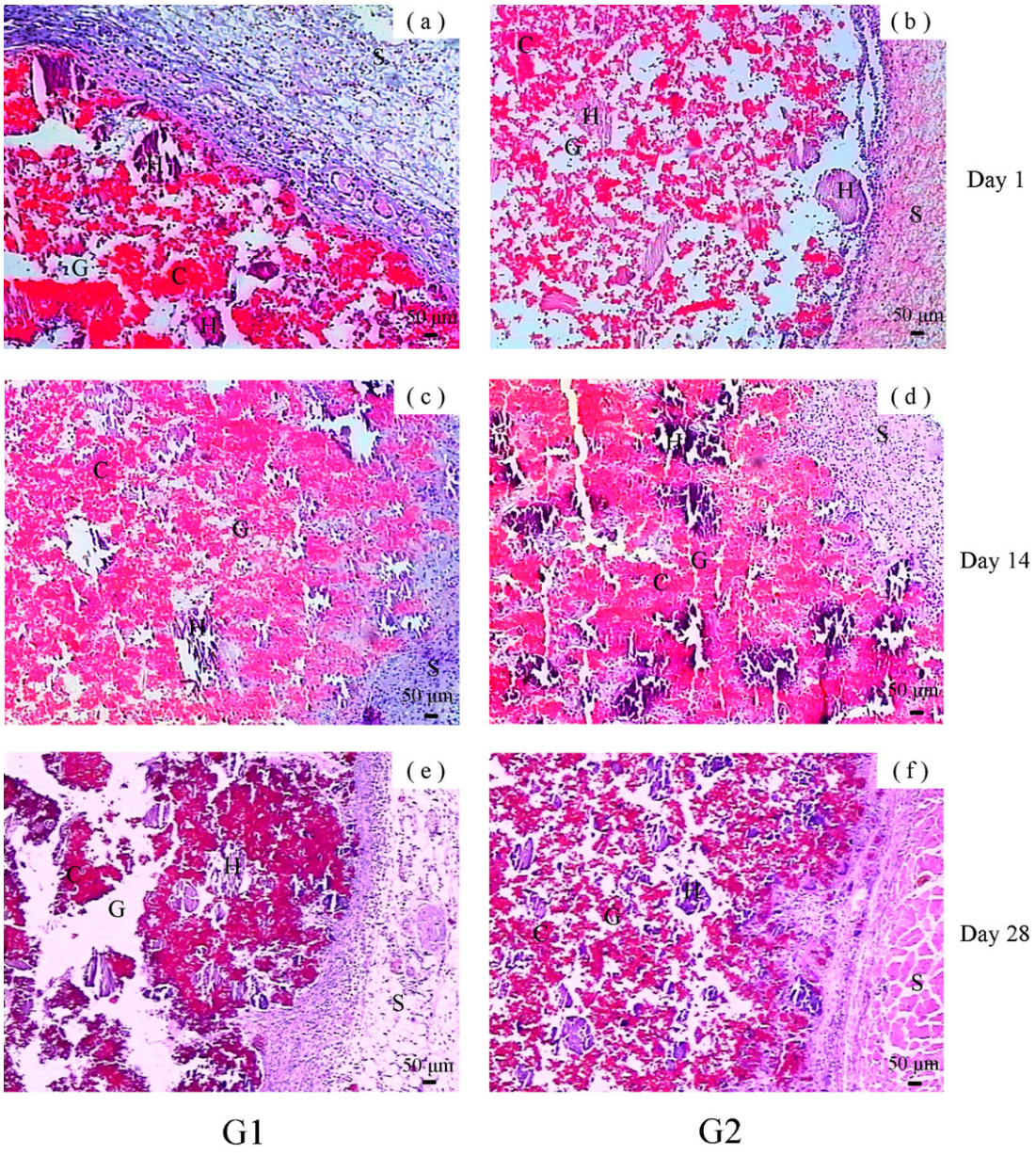

Fig. 7. Hematoxylin and eosin stained sections of the G1 gel (a, c and e) without rBMSCs and G2 gel (b, d and f) with rBMSCs after subcutaneous injection in rats on day 1 (a and b), day 14 (c and d) and day 28(e and f). G: gel; S: surrounding tissues; H: HA/Col; C: chitosan. Magnification: 40×.

4. Conclusions

The CS/HA/Col system showed a temperature-dependent phase-transition with a physiologically acceptable pH change. After gelation, the CS/HA/Col gel showed good mechanical stability, which might be due to the association between HA/Col and chitosan. Furthermore, the CS/HA/Col gel showed good cytocompatibility with rBMSCs. When the CS/HA/Col solution and rBMSCs were co-injected into the subcutaneous dorsum of the rats, rBMSCs survived inside the gel at the injection site for at least 28 days and improved the biocompatibility of the CS/HA/Col gels. In summary, the biocompatibility, cytocompatibility, phasetransition process, and rheological property made the CS/HA/Col system suitable as a delivery vehicle for rBMSCs.

Acknowledgements

The authors are grateful for the financial support from the 973 Project (2007CB815600), National Natural Science Foundation of China (51072090, 51061130554), and Natural Science Foundation of Guangdong Province, China (10451051501004727).

References

Ahn, H. H., Kim, K. S., Lee, J. H., Lee, J. Y., Kim, B. S., Lee, I. W., et al. (2009). In vivo osteogenic differentiation of human adipose-derived stem cells in an injectable in situ-forming gel scaffold. *Tissue Engineering Part A*, *15*(7), 1821–1832.

Akahane, M., Ohgushi, H., Yoshikawa, T., Sempuku, T., Tamai, S., Tabata, S., et al. (1999). Osteogenic phenotype expression of allogeneic rat marrow cells in porous hydroxyapatite ceramics. *Journal of Bone and Mineral Research*, *14*(4), 561–568.

Anderson, J. M. (2001). Biological responses to materials. *Annual Review of Materials Research*, *31*, 81–110.

Anseth, K. S., Bowman, C. N., & BrannonPeppas, L. (1996). Mechanical properties of hydrogels and their experimental determination. *Biomaterials*, *17*(17), 1647–1657.

Axelsson, J. B. F., Akbarshahi, H., Said, K., Malmstrom, A., & Andersson, R. (2010). Proposed protective mechanism of the pancreas in the rat. *Journal of Inflammation-London*, *7*.

Bartholomew, A., Sturgeon, C., Siatskas, M., Ferrer, K., McIntosh, K., Patil, S., et al. (2002). Mesenchymal stem cells suppress lymphocyte proliferation in vitro and prolong skin graft survival in vivo. *Experimental Hematology*, *30*(1), 42–48.

Baruch, L., & Machluf, M. (2006). Alginate–chitosan complex coacervation for cell encapsulation: Effect on mechanical properties and on long-term viability. *Biopolymers*, *82*(6), 570–579.

Bryant, S. J., Anseth, K. S., Lee, D. A., & Bader, D. L. (2004). Crosslinking density influences the morphology of chondrocytes photoencapsulated in PEG hydrogels during the application of compressive strain. *Journal of Orthopaedic Research*, *22*(5), 1143–1149.

Chen, Z. G., Mo, X. M., He, C. L., & Wang, H. S. (2008). Intermolecular interactions in electrospun collagen–chitosan complex nanofibers. *Carbohydrate Polymers*, *72*(3), 410–418.

Chenite, A., Buschmann, M., Wang, D., Chaput, C., & Kandani, N. (2001). Rheological characterisation of thermogelling chitosan/glycerol-phosphate solutions. *Carbohydrate Polymers*, *46*(1), 39–47.

Cho, J., Heuzey, M. C., Begin, A., & Carreau, P. J. (2006). Effect of urea on solution behavior and heat-induced gelation of chitosan-beta-glycerophosphate. *Carbohydrate Polymers*, *63*(4), 507–518.

Cho, J. Y., Heuzey, M. C., Begin, A., & Carreau, P. J. (2005). Physical gelation of chitosan in the presence of beta-glycerophosphate: The effect of temperature. *Biomacromolecules*, *6*(6), 3267–3275.

Cho, M. H., Kim, K. S., Ahn, H. H., Kim, M. S., Kim, S. H., Khang, G., et al. (2008). Chitosan gel as an in situ-forming scaffold for rat bone marrow mesenchymal stem cells in vivo. *Tissue Engineering Part A*, *14*(6), 1099–1108.

Dawson, E., Mapili, G., Erickson, K., Taqvi, S., & Roy, K. (2008). Biomaterials for stem cell differentiation. *Advanced Drug Delivery Reviews*, *60*(2), 215–228.

Di Nicola, M., Carlo-Stella, C., Magni, M., Milanesi, M., Longoni, P. D., Matteucci, P., et al. (2002). Human bone marrow stromal cells suppress T-lymphocyte proliferation induced by cellular or nonspecific mitogenic stimuli. *Blood*, *99*(10), 3838–3843.

Djouad, F., Plence, P., Bony, C., Tropel, P., Apparailly, F., Sany, J., et al. (2003). Immunosuppressive effect of mesenchymal stem cells favors tumor growth in allogeneic animals. *Blood*, *102*(10), 3837–3844.

Drury, J. L., & Mooney, D. J. (2003). Hydrogels for tissue engineering: Scaffold design variables and applications. *Biomaterials*, *24*(24), 4337–4351.

Hou, Q. P., De Bank, P. A., & Shakesheff, K. M. (2004). Injectable scaffolds for tissue regeneration. *Journal of Materials Chemistry*, *14*(13), 1915–1923.

Huang, Z., Feng, Q., Yu, B., & Li, S. (2011). Biomimetic properties of an injectable chitosan/nano-hydroxyapatite/collagen composite. *Materials Science and Engineering: C*, *31*(3), 683–687.

Ji, Q. X., Deng, J., Xing, X. A. M., Yuan, C. Q., Yu, X. B., Xu, Q. C., et al. (2010). Biocompatibility of a chitosan-based injectable thermosensitive hydrogel and its effects on dog periodontal tissue regeneration. *Carbohydrate Polymers*, *82*(4), 1153–1160.

Kim, K. S., Lee, J. H., Ahn, H. H., Lee, J. Y., Khang, G., Lee, B., et al. (2008). The osteogenic differentiation of rat muscle-derived stem cells in vivo within in situ-forming chitosan scaffolds. *Biomaterials*, *29*(33), 4420–4428.

Kloxin, A. M., Kloxin, C. J., Bowman, C. N., & Anseth, K. S. (2010). Mechanical properties of cellularly responsive hydrogels and their experimental determination. *Advanced Materials*, *22*(31), 3484–3494.

Lavertu, M., Filion, D., & Buschmann, M. D. (2008). Heat-induced transfer of protons from chitosan to glycerol phosphate produces chitosan precipitation and gelation. *Biomacromolecules*, *9*(2), 640–650.

Lessard, D. G., Ousalem, M., Zhu, X. X., Eisenberg, A., & Carreau, P. J. (2003). Study of the phase transition of poly(N,N-diethylacrylamide) in water by rheology and dynamic light scattering. *Journal of Polymer Science Part B-Polymer Physics*, *41*(14), 1627–1637.

Li, X. M., & Feng, Q. L. (2005a). Dynamic rheological behaviors of the bone scaffold reinforced by chitin fibres. In *Pricm 5: The Fifth Pacific Rim International Conference on Advanced Materials and Processing, Pts 1–5, 475–479* (pp. 2387–2390).

Li, X. M., & Feng, Q. L. (2005b). Porous poly-L-lactic acid scaffold reinforced by chitin fibers. *Polymer Bulletin*, *54*(1–2), 47–55.

Li, X. M., Feng, Q. L., Wang, W. J., & Cui, F. Z. (2006). Chemical characteristics and cytocompatibility of collagen-based scaffold reinforced by chitin fibers for bone tissue engineering. *Journal of Biomedical Materials Research Part B-Applied Biomaterials*, *77B*(2), 219–226.

Ma, G. P., Yang, D. Z., Li, Q. Z., Wang, K. M., Chen, B. L., Kennedy, J. F., et al. (2010). Injectable hydrogels based on chitosan derivative/polyethylene glycol dimethacrylate/N,N-dimethylacrylamide as bone tissue engineering matrix. *Carbohydrate Polymers*, *79*(3), 620–627.

Muzzarelli, R. A. A. (2009). Chitins and chitosans for the repair of wounded skin, nerve, cartilage and bone. *Carbohydrate Polymers*, *76*(2), 167–182.

Ohgushi, H., Goldberg, V. M., & Caplan, A. I. (1989). Heterotopic osteogenesis in porous ceramics induced by marrow-cells. *Journal of Orthopaedic Research*, *7*(4), 568–578.

Palmer, L. C., Newcomb, C. J., Kaltz, S. R., Spoerke, E. D., & Stupp, S. I. (2008). Biomimetic systems for hydroxyapatite mineralization inspired by bone and enamel. *Chemical Reviews*, *108*(11), 4754–4783.

Sionkowka, A., Wisniewski, M., Skopinska, J., Kennedy, C. J., & Wess, T. J. (2004). Molecular interactions in collagen and chitosan blends. *Biomaterials*, *25*(5), 795–801.

Weiner, S., & Wagner, H. D. (1998). The material bone: Structure mechanical function relations. *Annual Review of Materials Science*, *28*, 271–298.

Yoshikawa, T., Ohgushi, H., & Tamai, S. (1996). Immediate bone forming capability of prefabricated osteogenic hydroxyapatite. *Journal of Biomedical Materials Research*, *32*(3), 481–492.

Zhang, W., Liao, S. S., & Cui, F. Z. (2003). Hierarchical self-assembly of nano-fibrils in mineralized collagen. *Chemistry of Materials*, *15*(16), 3221–3226.

Zhao, Q. S., Ji, Q. X., Xing, K., Li, X. Y., Liu, C. S., & Chen, X. G. (2009). Preparation and characteristics of novel porous hydrogel films based on chitosan and glycerophosphate. *Carbohydrate Polymers*, *76*(3), 410–416.